


# Event activity measurements and mid-rapidity correlations in 200 GeV p+Au collisions at STAR<sup>†</sup>

David Stewart <sup>1</sup>  for the STAR Collaboration

<sup>1</sup> Yale University; david.j.stewart@yale.edu

<sup>†</sup> Presented at Hot Quarks 2018 - Workshop for young scientists on the physics of ultrarelativistic nucleus-nucleus collisions, Texel, The Netherlands, September 7-14 2018

Version January 11, 2019 submitted to Proceedings

**Abstract:** These proceedings report preliminary measurements of correlations between mid-rapidity charged tracks and high-rapidity event activity (EA) at STAR for  $\sqrt{s_{NN}} = 200$  GeV p+Au collisions taken in 2015. These correlations are intriguing because they inform the current debate over use of the Glauber model in “small” systems (here meaning p+A or d+A and denoted as “s+A”) and have implications for calculating nuclear modification and quenching observables in these systems. The results support concerns about centrality binning in p+Au collisions, and as such motivate using ratios of semi-inclusive, as opposed to fully inclusive, jet spectra to look for jet enhancement or suppression.

**Keywords:** STAR; jet; p+Au; RAA; suppression; small systems; 200GeV; Ncoll; event activity

## 1. Introduction

The statistical distributions of binary nucleon-nucleon collisions in A+A collisions ( $N_{\text{coll}}$ ), calculated by the Glauber Model [1], as a function of impact parameter  $b$ , play an important role in probing nuclear modification in A+A collisions. The  $N_{\text{coll}}$  distributions are binned into centrality classes. In each distribution,  $N_{\text{coll}}$  is maximum for the most central bin, i.e. with  $b \rightarrow 0$ , and decreases monotonically through the most peripheral bin. The results of hard scatterings are compared in ratio to those from p+p collisions scaled by  $N_{\text{coll}}$ . For jets, the deviation of this ratio ( $R_{AA}^{\text{jet}}$ ) from unity is an indication of nuclear modification. In A+A events, the strong suppression of  $R_{AA}^{\text{jet}}$  is an indicator of quark gluon plasma (QGP) formation. The traditional assumption was that small systems would not form a QGP. Therefore,  $R_{sA}^{\text{jet}}$  was measured in order to study cold nuclear matter effects.

The first inclusive measurements of  $R_{sA}^{\text{jet}}$  were reported for 5.02 TeV p+Pb collisions at the LHC by ALICE [2], CMS [3], and ATLAS [4], and for 200 GeV d+Au collisions at PHENIX at RHIC [5]. As expected, the values of  $R_{sA}^{\text{jet}}$ , when not binned into centrality classes, were consistent with unity. However, centrality binned  $R_{sA}^{\text{jet}}$  showed significant suppression/enhancement for central/peripheral collisions at both ATLAS and PHENIX, a similar result to that interpreted as a QGP signal in A+A collisions. Tantalizingly, this coincided with larger community interest in small systems as a variety of particle collectivity signals were observed in s+A collisions.

## 2. Event activity estimation and correlations to $R_{sA}^{\text{jet}}$

Calculating  $R_{AA}^{\text{jet}}$  assumes that the probability of a hard scattering scales linearly with  $N_{\text{coll}}$ , which is applied to collisions by assuming that it scales monotonically with a measured event activity estimation ( $EA_{\text{est}}$ ). In the above measurements,  $EA_{\text{est}}$  values were determined by detectors at  $\eta$  values outside of the region where the jets were reconstructed in order to avoid auto-correlations between  $EA_{\text{est}}$  and  $R_{sA}^{\text{jet}}$ .

The observed suppression/enhancement of  $R_{sA}^{\text{jet}}$  may artificially result from difficulties applying  $N_{\text{coll}}$  which are unique to small systems. First, compared to A+A collisions, small systems have large fluctuations in  $EA_{\text{est}}$  coupled with a relatively limited range of  $N_{\text{coll}}$ . This can result in a dynamical bias when calculating  $R_{sA}^{\text{jet}}$  [6]. More intriguing is the possibility that individual nucleon-nucleon collisions within a single s+A collision that share a common nucleon are not independent. The effects of such a correlation would be strongly evident in a p+A collision relative to an A+A collision. In the former, every nucleon-nucleon collision shares the same proton; in the latter many independent sets of such collisions would be superimposed, thereby masking the effects of the correlation.

A study of p+Pb collisions at LHC energies concluded that a 20% suppression of soft particles correlated with the presence of a hard scattering would reproduce the enhancement/suppression observed in  $R_{sA}^{\text{jet}}$  [7]. Energy conservation of a proton (or deuteron) common to a set of nucleon-nucleon collisions may provide the physics mechanism for this correlation. Jet production would require a hard scattering in one nucleon-nucleon collision, and therefore a reduction in energy available for the production of soft particles in the remaining collisions. Two such theory calculations found this to be a sufficient explanation for the observed suppression of central  $R_{sA}^{\text{jet}}$ , one of which also found it sufficient for the peripheral enhancement [8][9].

### 3. Correlations of $EA_{\text{est}}$ to mid-rapidity charged tracks at STAR for p+Au collisions

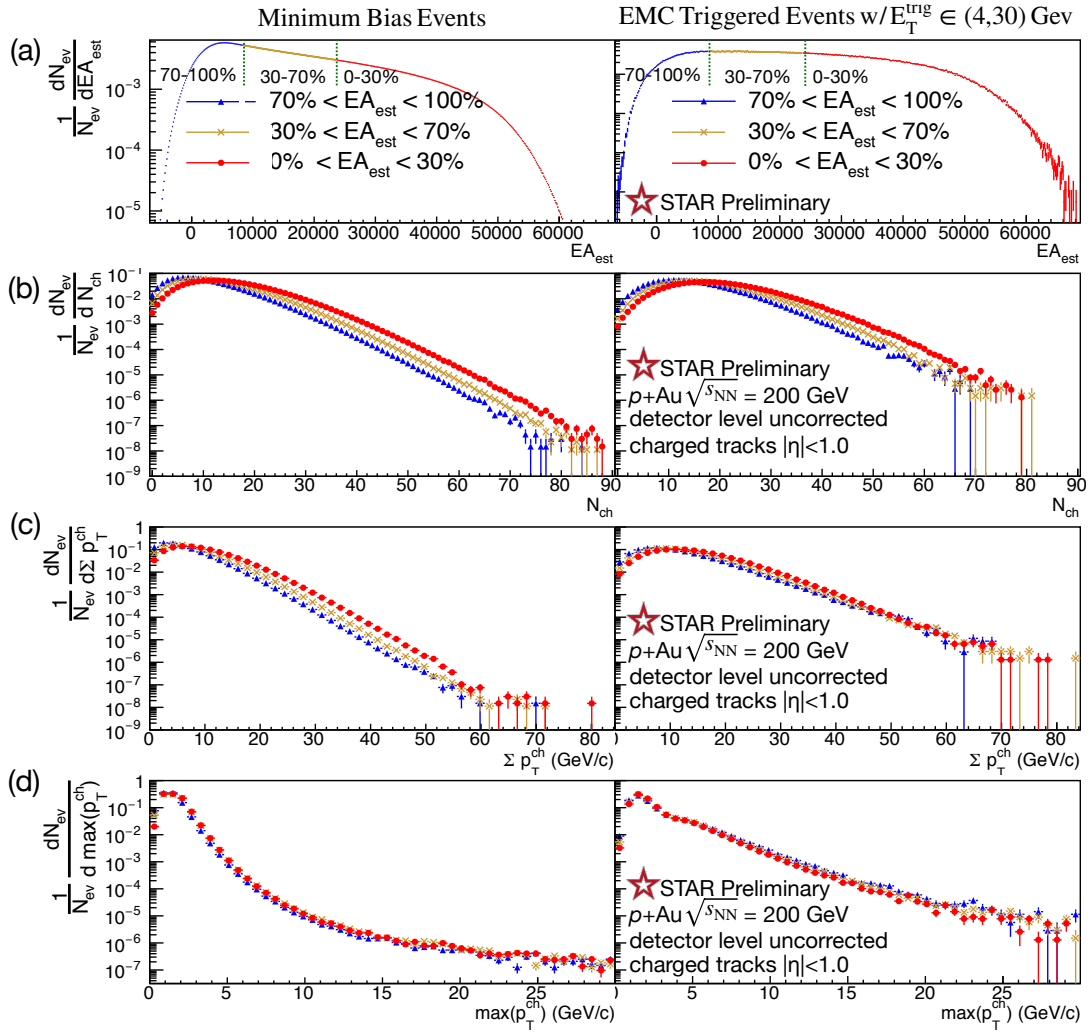
STAR has a large set of  $\sqrt{s_{\text{NN}}} = 200$  GeV p+Au collisions recorded in 2015 which will help address questions raised by the jet measurements already released by PHENIX and the LHC experiments. Measurements of mid-rapidity charged track correlations to high- $\eta$   $EA_{\text{est}}$ , presented in Figure 1 and Figure 2, clearly indicate that further study is required prior to calculating the  $R_{sA}^{\text{jet}}$ .

The figures present data from events with two separate triggers. First: minimum bias (MB) events. Second: events triggered by the electromagnetic calorimeter (EMC) selected by the hit with the maximum transverse energy ( $E_{\text{T}}^{\text{trig}}$ ). The correlations reported are for charged tracks measured in the time projection chamber (TPC) which has good track resolution from 0.2 to 30 GeV/c and has, as does the EMC, full azimuthal coverage.  $EA_{\text{est}}$  is measured as the sum of the signal in the inner ring of the beam beam counter (BBC) in the Au-going direction. The BBC consists of sets of plastic scintillators arrayed around the beam pipe; the inner ring of which covers rapidity range 3.3 to 5.8.

These preliminary results are detector level and uncorrected for detector acceptance or inefficiency effects. However, the conclusions presented depend on the data's monotonicity and relative distributions and are consequently not sensitive to detector tracking efficiencies and pileup. Statistical uncertainties are plotted for all data. Additionally, a small relative trigger bias is added in quadrature with the statistical uncertainty in Figure 2 (a2), (b), and (c). This bias is quantified by the difference in results from the MB data when cut for EMC hits so as to mimic the EMC trigger and the results from the actual EMC triggered data.

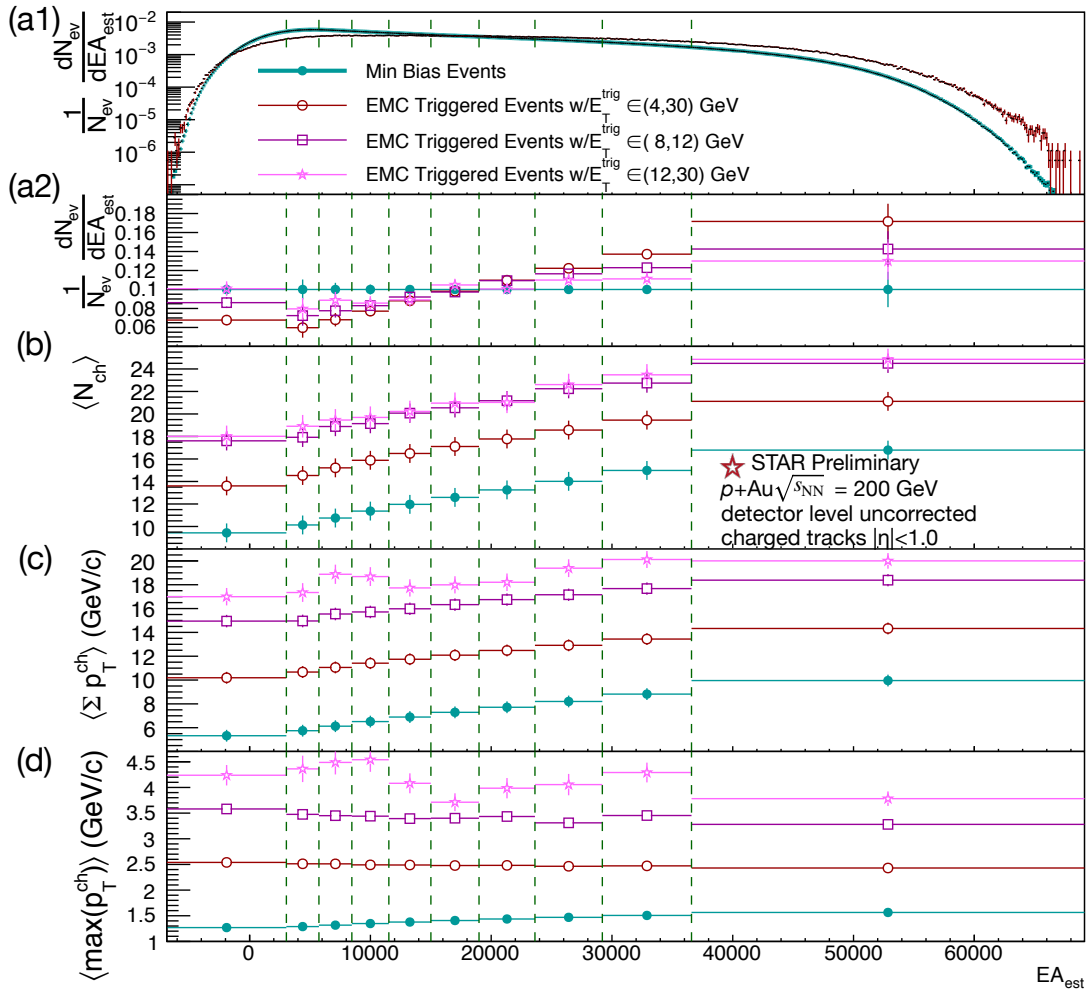
Figure 1 (a) shows the  $EA_{\text{est}}$  distributions for MB events (on left) and EMC triggered events (on right). As in the case of centrality in Glauber calculations,  $EA_{\text{est}}$  percentiles are defined by the MB distribution with 100% being the lowest and 0% the highest value. Here the  $EA_{\text{est}}$  distribution is divided into low (100-70%), medium (30-70%), and high (0-30%) activity bins. For each  $EA_{\text{est}}$  bin, the distribution of multiplicity, summed  $p_{\text{T}}$ , and maximum single track  $p_{\text{T}}$ , are given in (b), (c), and (d). Compared to A+A collisions, the distributions in p+Au collisions heavily overlap among  $EA_{\text{est}}$  bins. As expected, the mean values of multiplicity and summed track  $p_{\text{T}}$  are higher for the high  $EA_{\text{est}}$  bins. The normalization of the curves in (d) is dominated by the first few, low- $p_{\text{T}}$ , bins. In these bins the spectra from high, medium, and low  $EA_{\text{est}}$  events are fairly comparable. After these low  $p_{\text{T}}$  bins, the spectrum of each  $EA_{\text{est}}$  bin continues to be roughly equivalent for harder scatterings in the MB data; however, for the EMC triggered data, the high  $EA_{\text{est}}$  bin's spectrum is somewhat suppressed relative to the low  $EA_{\text{est}}$  bin's spectrum.

Figure 2 (a1) gives the same  $EA_{\text{est}}$  distributions (MB and EMC triggered) shown in Figure 1 (a). The  $EA_{\text{est}}$  binning, consistent between all plots, is selected for uniform numbers of MB events. The



**Figure 1.** Correlations between charged tracks at STAR ( $|\eta| < 1$ ) and  $EA_{est}$ , the Au-going BBC inner ring signal ( $|\eta| \in (3.3, 5.8)$ ). (a) left:  $EA_{est}$  distribution of MB events, binned for the maximum and minimum 30% as well as the middle 40% of events. (a) right: distribution of  $EA_{est}$  in for EMC triggered events; the binning boundaries and labels are determined by the MB distribution. Columns (b), (c), and (d) give the distributions for the low, mid, and high  $EA_{est}$  bins for charged track multiplicity, summed  $p_T$ , and maximum  $p_T$  respectively.

remaining panels plot average (a2) (normalized) number of events, (b) multiplicity, (c) summed track  $p_T$ , and (d) maximum single track  $p_T$ . The results of two subsets of the EMC data, with higher trigger thresholds, are also plotted. The most striking results are deviations from what would result if  $EA_{est}$  and  $N_{coll}$  scaled positively, monotonically, together. If true, that scaling would result in correlations in (a2)-(d) that are: (1) positive, except, of course, for MB events in (a2), and, (2) smallest for MB events and successively larger for EMC triggered events with successively higher trigger thresholds. Instead, while each correlation is positive in (a2), the correlations are smaller for each successively higher  $E_T^{trig}$  threshold; the data is too limited for harder triggers to see if there would be an actual turnover at a sufficiently high threshold. Correlations in (c) and (d) are about as naively expected, although it is curious that mean multiplicity and summed  $p_T$  appear relatively saturated by the time there is an 8 GeV  $E_T^{trig}$  such that they increase only slightly with the higher 12 GeV threshold. Most notably, each EMC triggered distribution (d) is anti-correlated; this directly contradicts the assumption that hard scatterings (and therefore naively higher  $E_T^{trig}$  values) scale linearly with  $EA_{est}$ .



**Figure 2.** Correlations between charged tracks at STAR ( $|\eta| < 1$ ) and  $EA_{\text{est}}$ , the Au-going BBC inner ring signal ( $|\eta| \in (3.3, 5.8)$ ). Each panel is plotted with data from MB events as well EMC  $E_T^{\text{trig}}$  triggered events. (a) The number of events of each BBC bin; each bin's boundaries are selected to contain 10% of the MB data. (b) Average number of charged tracks per event. (c) Average sum of  $p_T$  per event. (d) Average maximum track  $p_T$  per event.

#### 4. Summary

Correlations of mid rapidity charged track observables to high  $\eta$   $EA_{\text{est}}$  have been presented. The results imply challenges to the use of  $EA_{\text{est}}$  to determine associated  $N_{\text{coll}}$  values. These difficulties motivate the use of semi-inclusive jet spectra, in which  $N_{\text{coll}}$  cancels in the ratio, instead of fully inclusive spectra, to probe for jet suppression/enhancement in p+Au collisions [10][11].

**Funding:** This research was funded by U.S. Department of Energy under grant number DE-SC004168.

#### References

1. G. David, PoS **INPC2016**, 345 (2017).
2. J. Adam et al. (ALICE), Eur. Phys. J. **C76**, 271 (2016).
3. V. Khachatryan et al. (CMS), Eur. Phys. J. **C76**, 372 (2016).
4. G. Aad et al. (ATLAS), Phys. Lett. **B748**, 392 (2015).
5. A. Adare et al. (PHENIX), Phys. Rev. Lett. **116**, 122301 (2016).
6. J. Adam et al. (ALICE), Phys. Rev. **C91**, 064905 (2015).
7. A. Bzdak, V. Skokov, and S. Bathe, Phys. Rev. **C93**, 044901 (2016).

8. N. Armesto, D. C. Gülhan, and J. G. Milhano, *Phys. Lett.* **B747**, 441 (2015).
9. M. Kordell and A. Majumder, *Phys. Rev.* **C97**, 054904 (2018).
10. S. Acharya et al. (ALICE), *Phys. Lett.* **B783**, 95 (2018).
11. L. Adamczyk et al. (STAR), *Phys. Rev.* **C96**, 024905 (2017).

© 2019 by the author. Submitted to *Proceedings* for possible open access publication under the terms and conditions of the Creative Commons Attribution (CC BY) license (<http://creativecommons.org/licenses/by/4.0/>).